

Prompt photon and Drell-Yan pair production in the k_T -factorization approach at modern colliders

M.A. Malyshev

in collaboration with

A.V. Lipatov

N.P. Zotov

M.V. Lomonosov Moscow State University
D.V. Skobeltsyn Institute of Nuclear Physics

Phys. Lett. **B 699** (2011) 93

Outline

1. Motivation
2. k_T -factorization approach
 - unintegrated parton distributions
 - off-shell matrix elements
3. Parameters
4. Numerical results
5. Conclusion

Motivation

Prompt photon and Drell-Yan pair production are highly sensitive to parton distribution in the hadron. So they provide a test of hard subprocess dynamics. Also these processes contribute largely into the background of the 'new physics'.

At LHC energies the studied processes are small- x physics processes. At small x one has to use the k_T -factorization approach. For prompt photon production this approach was used in [S.P. Baranov, A.V. Lipatov, N.P. Zotov, 2010].

Recently new experimental data on inclusive prompt photon and Drell-Yan pair production have been obtained at LHC. Here we present the theoretical description of the LHC results for prompt photon production. For Drell-Yan process we present the description of various published Tevatron data.

k_T -factorization approach

1. Unintegrated parton distributions
2. Matrix elements which depend on the transverse momenta of incoming partons.

Unintegrated parton distributions

1. KMR approach(Kimber, Martin, Ryskin) [M.A. Kimber, A.D. Martin, M.G. Ryskin, 2001; G. Watt, A.D. Martin, M.G. Ryskin, 2003]. Weakening of the DGLAP strong ordering:

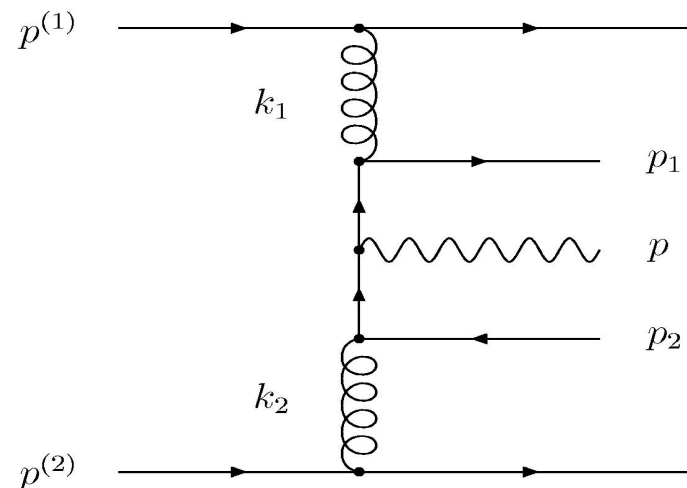
$$k_{1,T} \ll \dots \ll k_{n-1,T} \ll k_T \sim \mu$$

2. CCFM unintegrated distributions [H. Jung, 2004; M. Deak, H. Jung, K. Kutak, 2008]. Numerical solutions of CCFM equation. The starting distribution is chosen to satisfy proton structure function $F_2(x, \mu^2)$.

Off-shell matrix elements

I. Prompt photons

1. Compton subprocess $q^*g^* \rightarrow \gamma q$
2. Annihilation subprocess $q^*\bar{q}^* \rightarrow \gamma g$
3. Gluon fusion subprocess $g^*g^* \rightarrow \gamma q\bar{q}$ [S.P. Baranov, A.V. Lipatov, N.P. Zotov, 2008]. The taking into account of this higher order subprocess is not trivial in our approach.



Off-shell matrix elements

II. Drell-Yan

1. $q^* \bar{q}^* \rightarrow e^+ e^-$
2. $q^* \bar{q}^* \rightarrow e^+ e^- g$
3. $q^* g^* \rightarrow e^+ e^- q$

Parameters

- Significant theoretical uncertainties are connected with the choice of the factorization and renormalization scales. We took $\mu_R = \mu_F = \mu = \xi|\mathbf{p}_T|$ for prompt photons production and $\mu_R = \mu_F = \mu = \xi M_{e^+e^-}$ for Drell-Yan production.
- We varied the scale parameter ξ between 1/2 and 2 about the default value $\xi = 1$.
- We neglected the quarks masses.
- For completeness, we use LO formula for the strong coupling constant $\alpha_s(\mu^2)$ with $n_f = 4$ active quark flavours at $\Lambda_{\text{QCD}} = 200 \text{ MeV}$.

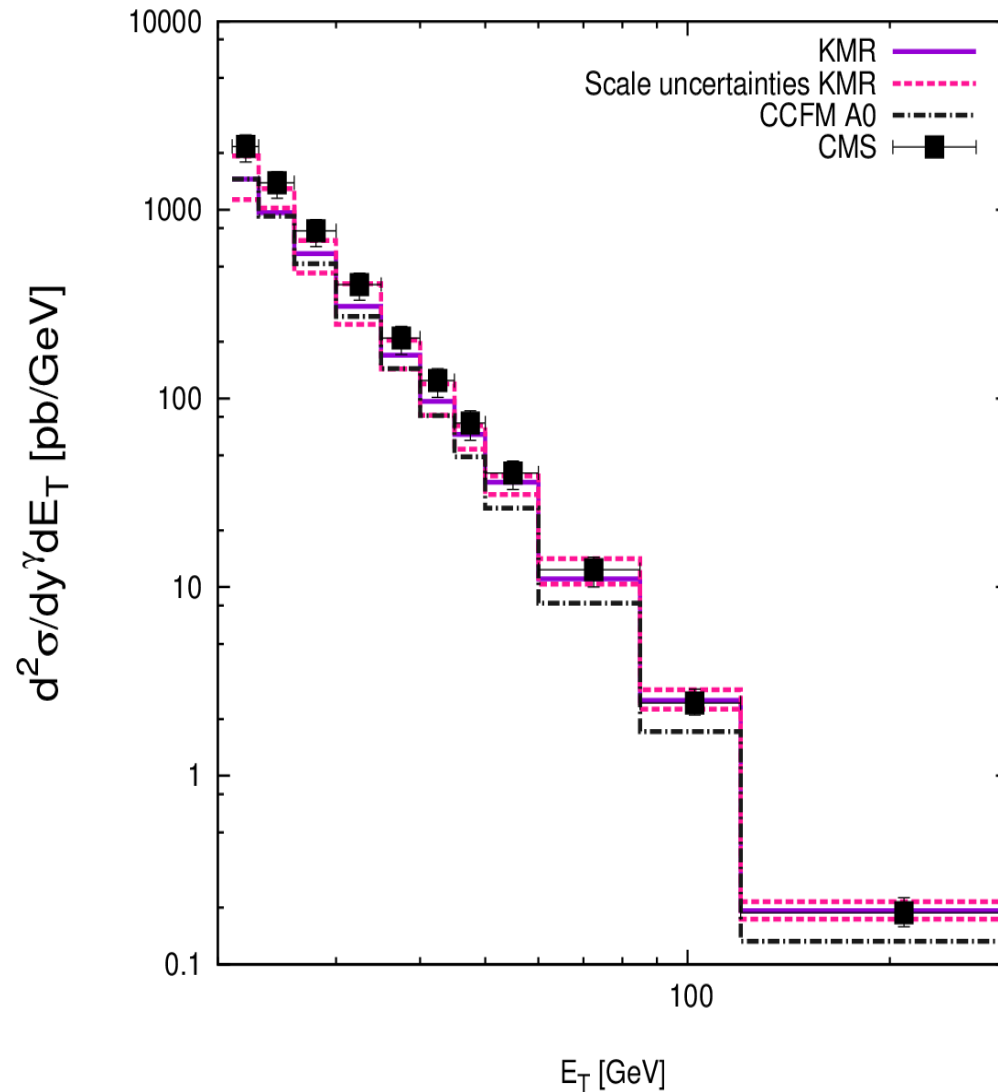
Parameters

In order to reduce the huge background from the secondary photons produced by the decays of π_0 and η mesons the isolation criterion is introduced in the experimental analyses. This criterion is the following. A photon is isolated if the amount of hadronic transverse energy E_T^{had} deposited inside a cone with aperture R centered around the photon direction in the pseudo-rapidity and azimuthal angle plane, is smaller than some value E^{max} .

$$E_T^{\text{had}} \leq E^{\text{max}}$$
$$(\eta^{\text{had}} - \eta)^2 + (\varphi^{\text{had}} - \varphi)^2 \leq R^2.$$

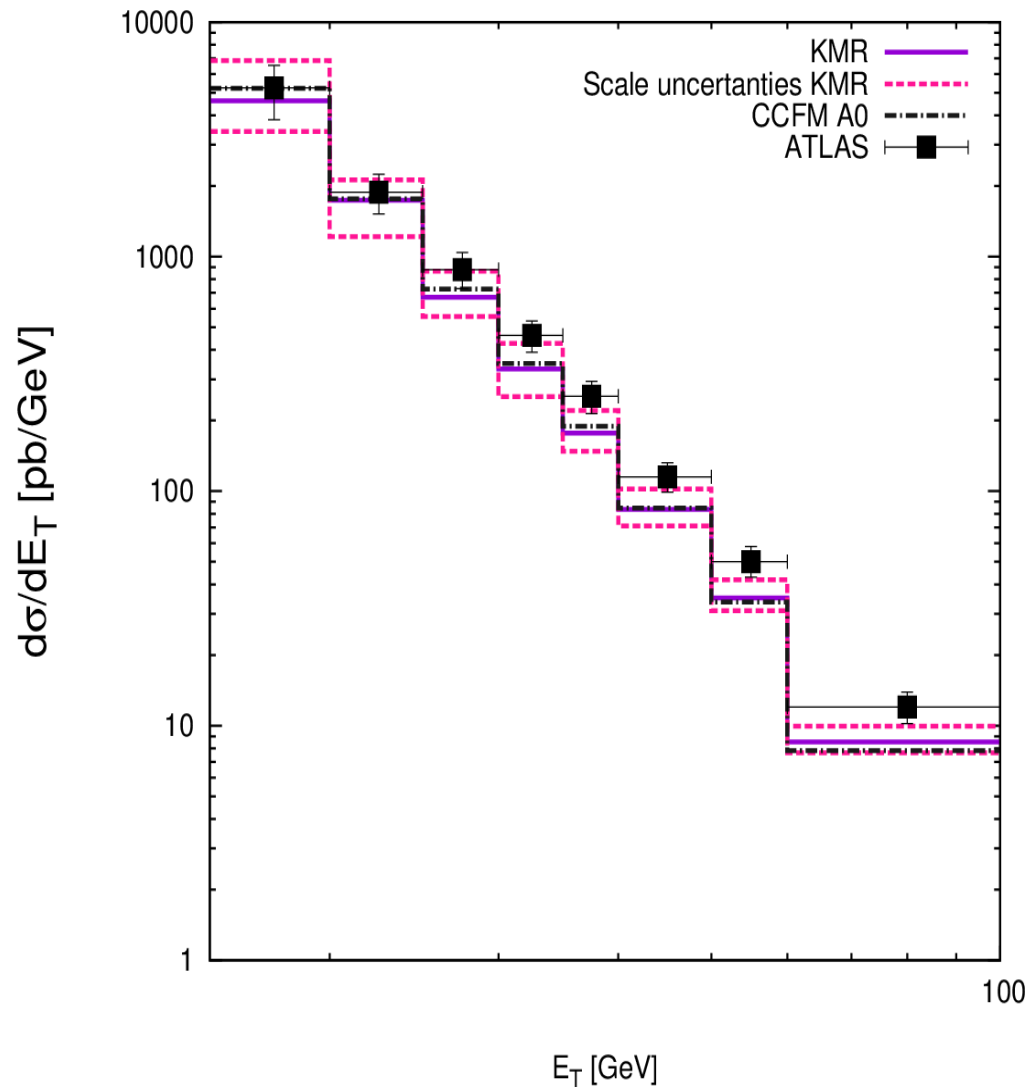
The isolation not only reduces the background but also significantly reduces the so called fragmentation components, connected with collinear photon radiation (10%). Both CMS and ATLAS collaborations take $R \sim 0.4$ and $E^{\text{max}} \sim 1$ GeV.

Numerical results



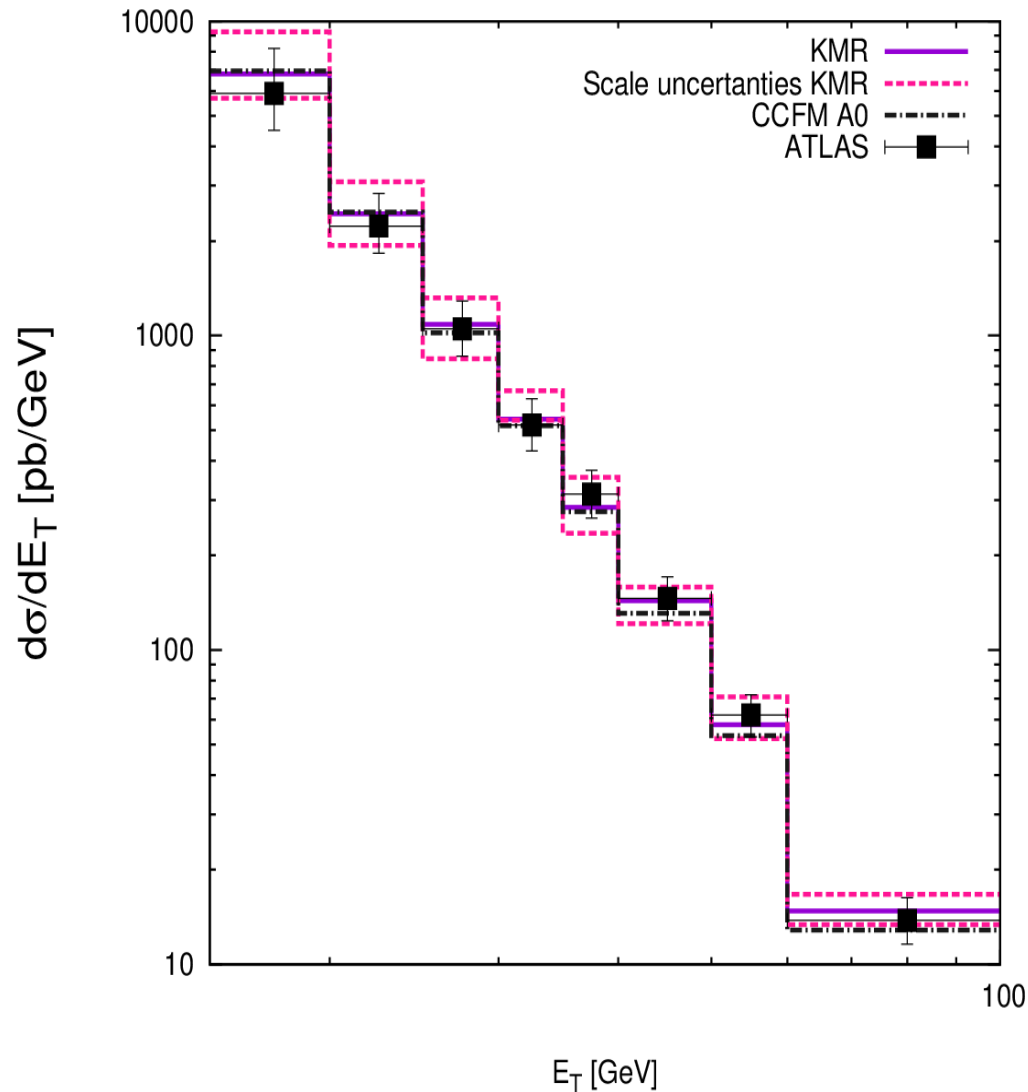
1. Differential cross section of inclusive prompt photon production $pp \rightarrow \gamma X$ at LHC energies ($\sqrt{S}=7$ TeV). The experimental data are of CMS ($|y| < 1,45$).

Numerical results



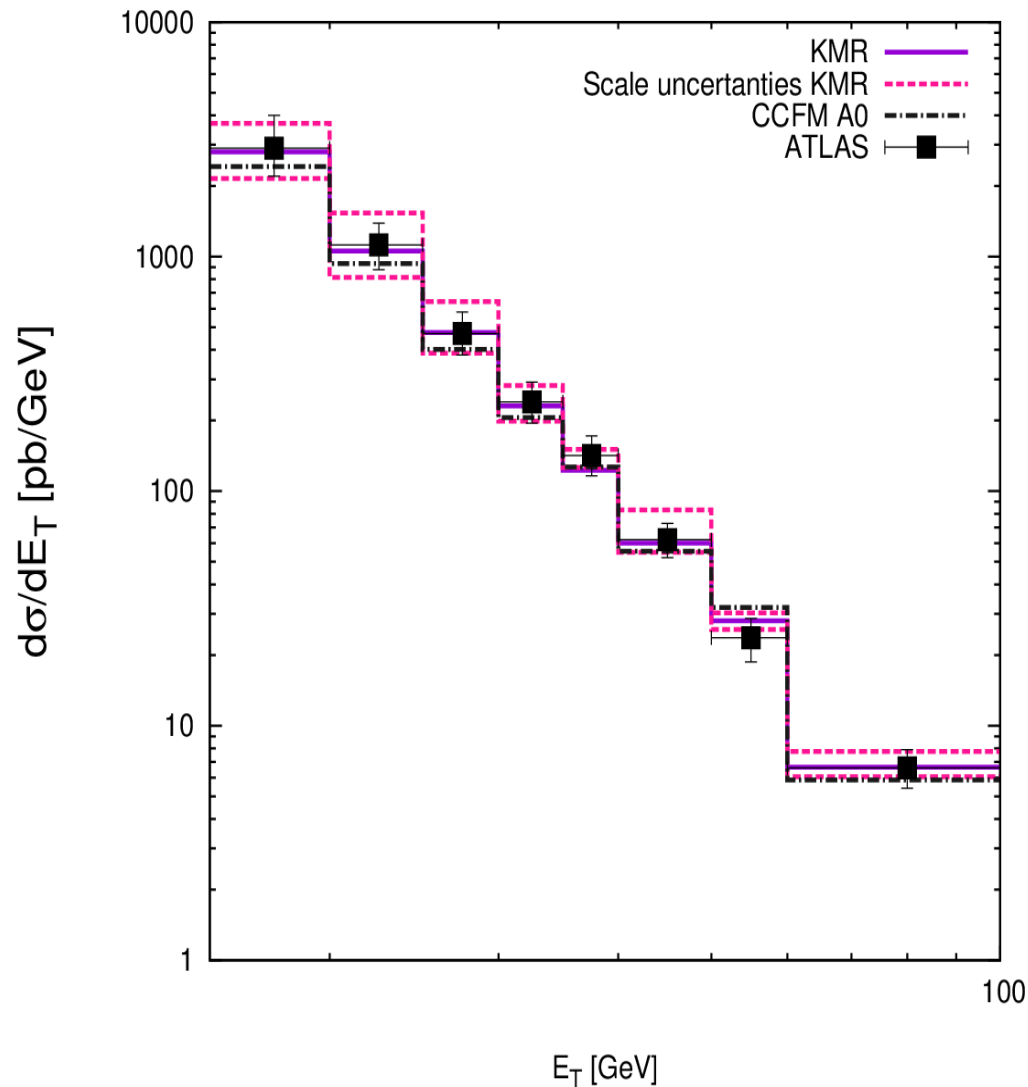
2. Differential cross section of inclusive prompt photon production $pp \rightarrow \gamma X$ at LHC energies ($\sqrt{S}=7$ TeV). The experimental data are of ATLAS ($|y| < 0,6$).

Numerical results



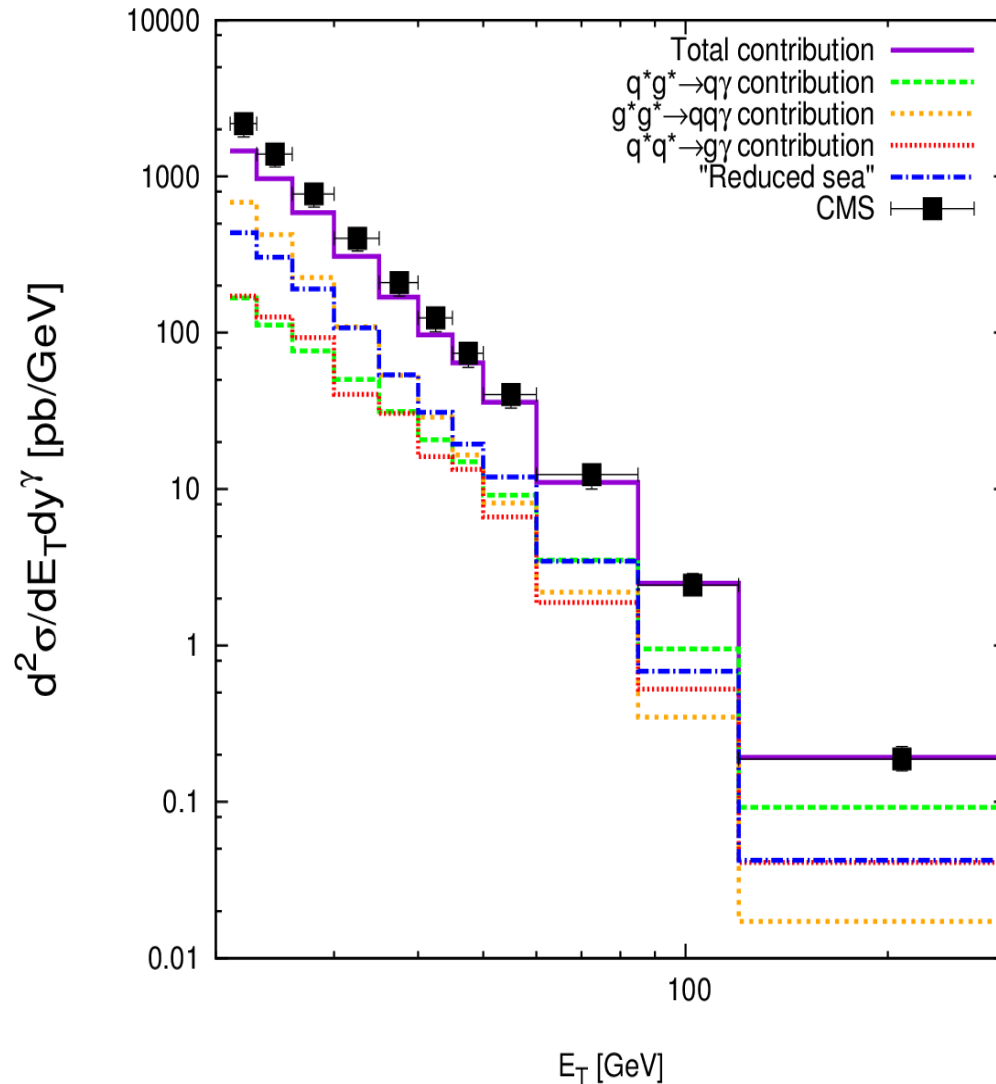
2. Differential cross section of inclusive prompt photon production $pp \rightarrow \gamma X$ at LHC energies ($\sqrt{S}=7$ TeV). The experimental data are of ATLAS ($0,6 < |y| < 1,37$).

Numerical results



2. Differential cross section of inclusive prompt photon production $pp \rightarrow \gamma X$ at LHC energies ($\sqrt{S}=7$ TeV). The experimental data are of ATLAS ($1.52 < |\eta| < 1.81$).

Numerical results

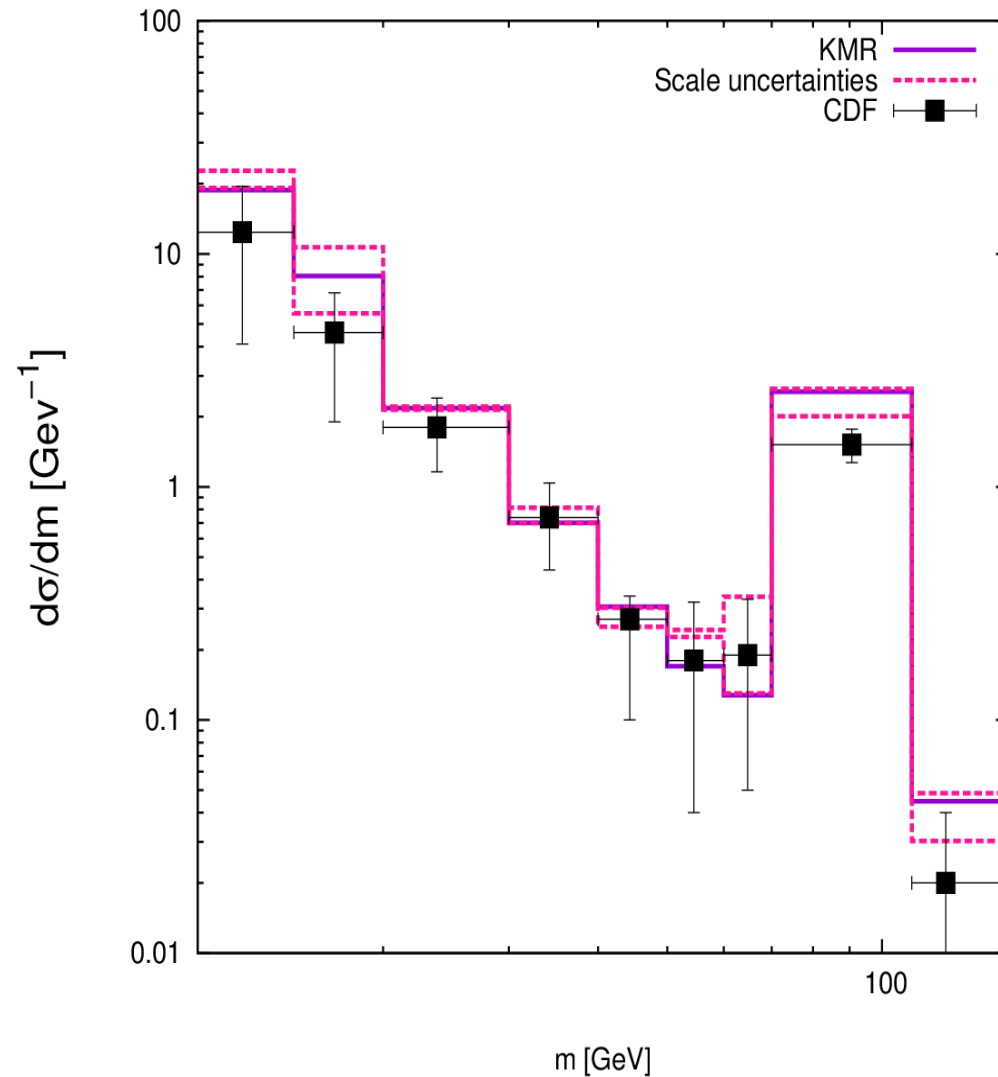


3. Differential cross section of inclusive prompt photon production $pp \rightarrow \gamma X$ at LHC energies ($\sqrt{S}=7$ TeV). Contribution of different subprocesses to the cross section, evaluated with KMR distributions. The experimental data are of CMS.

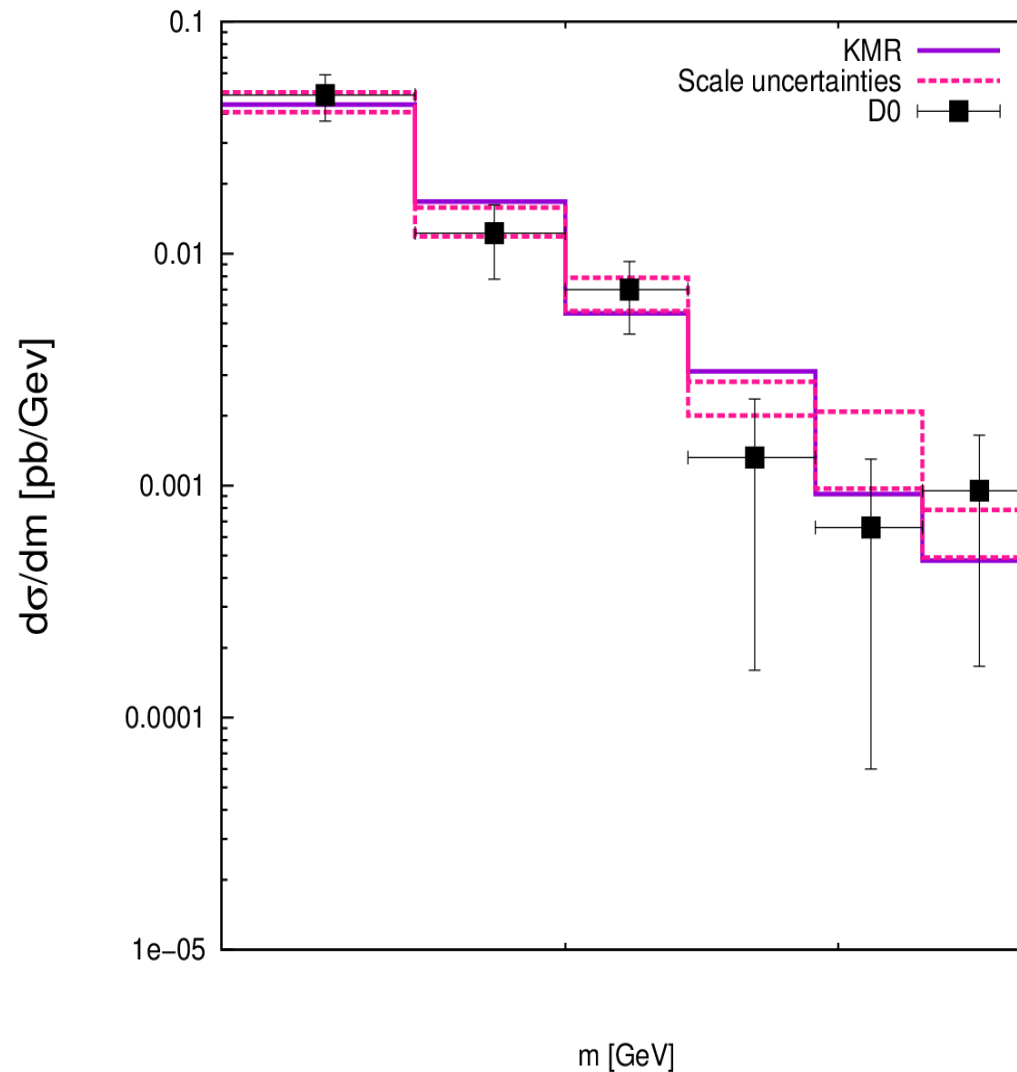
The $gg \rightarrow qq\gamma$ contribution is significant at the LHC energy, especially at low E_T

Numerical results

4. Differential cross section of Drell-Yan pair production $p\bar{p} \rightarrow e^+e^-X$ at Tevatron energies ($\sqrt{S}=1.8$ TeV) in the invariant masses range $11 < M < 150$ GeV. The experimental data are of CDF.



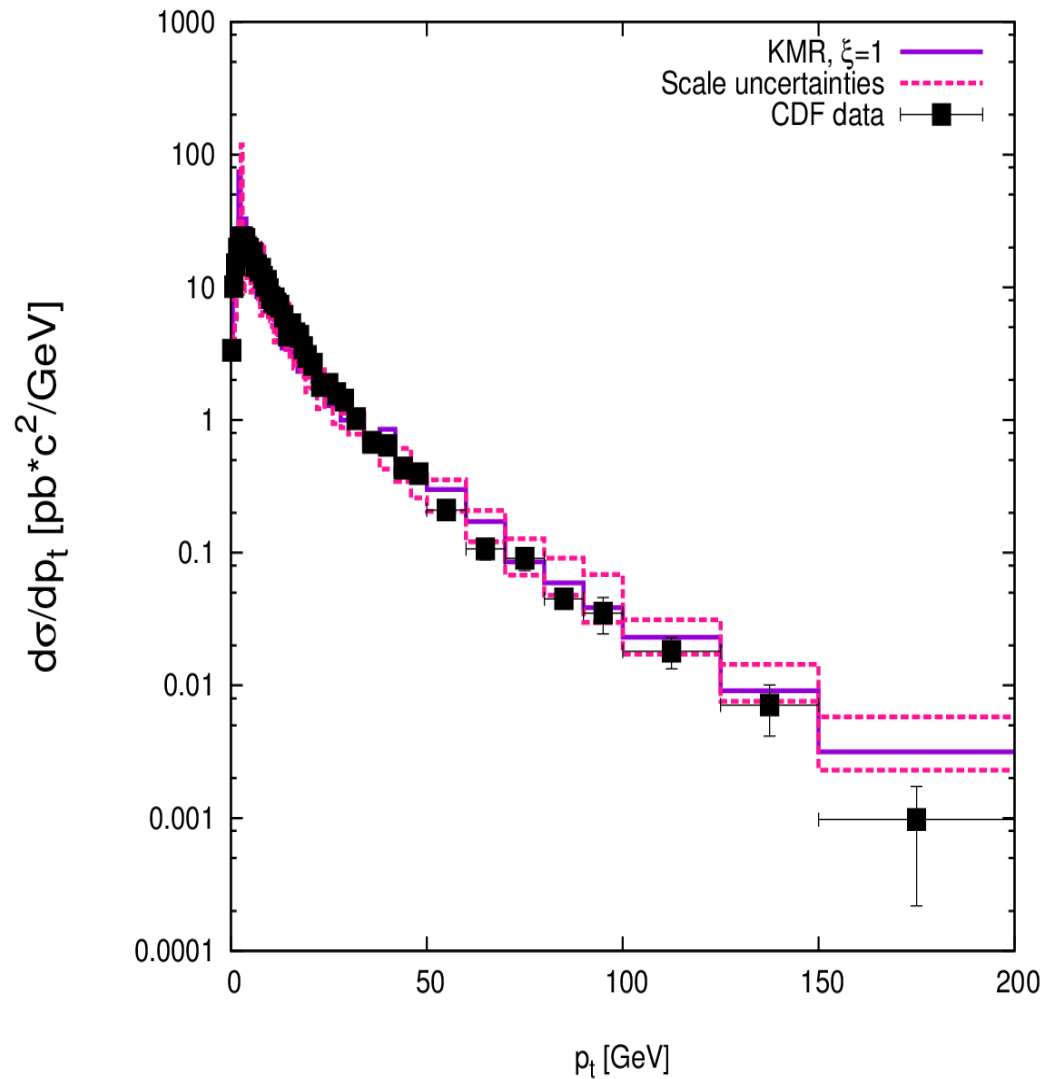
Numerical results



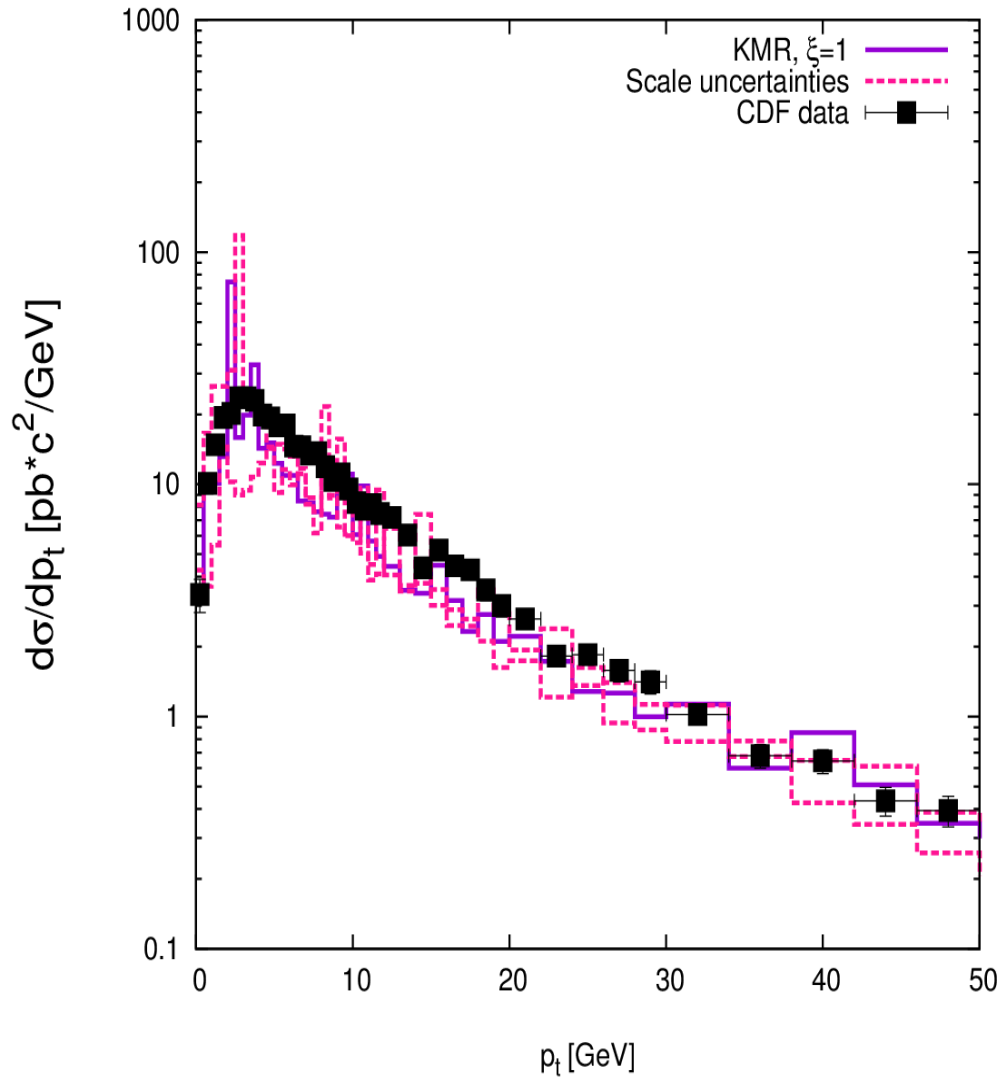
5. Differential cross section of Drell-Yan pair production $p\bar{p} \rightarrow e^+e^-X$ at Tevatron energies ($\sqrt{S}=1.8$ TeV) in the invariant masses range $120 < M < 400$ GeV. The experimental data are of D0.

Numerical results

6. Differential cross section of Drell-Yan pair production $p\bar{p} \rightarrow e^+e^-X$ at Tevatron energies ($\sqrt{S}=1.8$ TeV) versus the transverse momentum of the lepton pair. The experimental data are of CDF.



Numerical results



6. Differential cross section of Drell-Yan pair production $p\bar{p} \rightarrow e^+e^-X$ at Tevatron energies ($\sqrt{S}=1.8$ TeV) versus the transverse momentum of the lepton pair (in the range $0 < p_T < 50$ GeV). The experimental data are of CDF.

Conclusion

In the presented work processes of the inclusive prompt photon and Drell-Yan pair production in the k_T -factorization QCD approach at Tevatron and LHC energies have been studied.

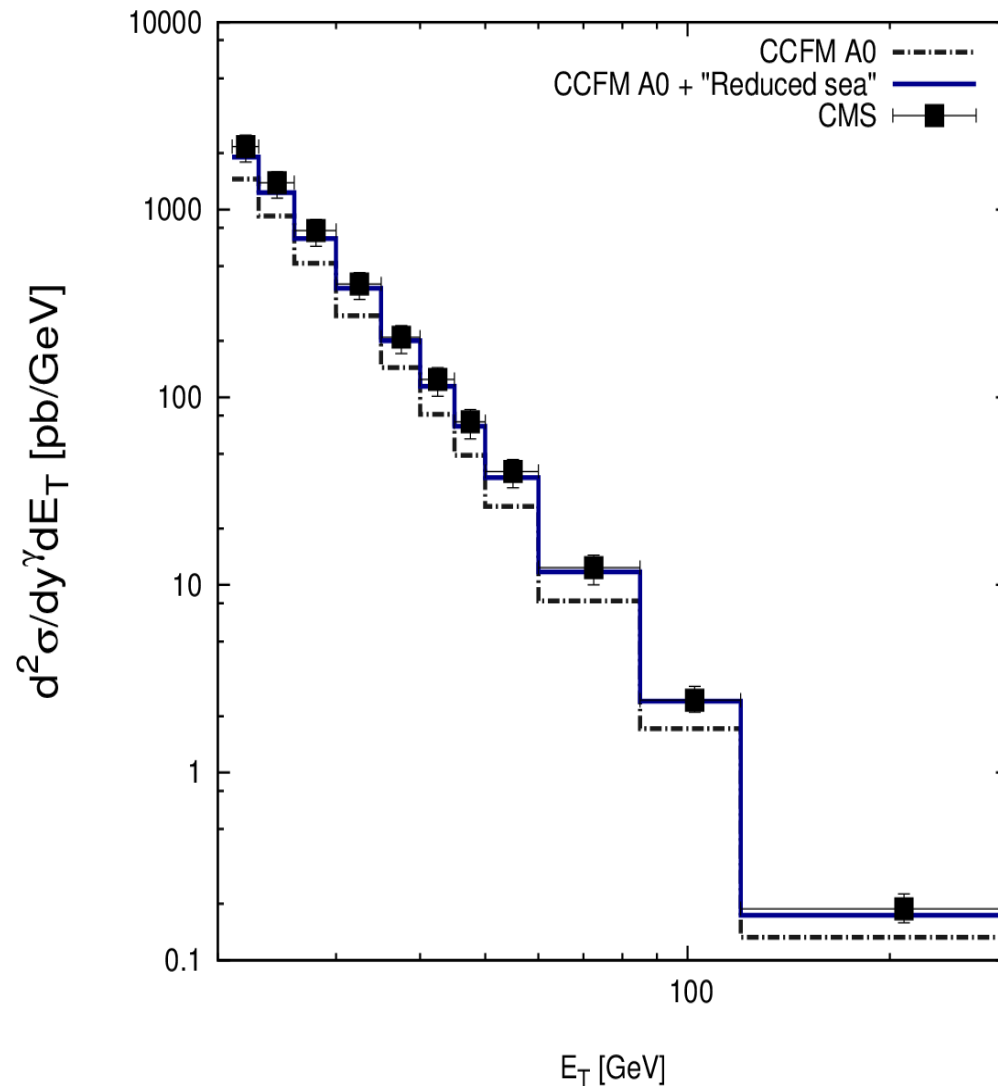
The off-shell LO matrix elements for $q^*g^* \rightarrow \gamma q$, $q^*\bar{q}^* \rightarrow \gamma g$, $q^*\bar{q}^* \rightarrow e^+e^-$ and HO matrix elements for $g^*g^* \rightarrow \gamma q\bar{q}$, $q^*\bar{q}^* \rightarrow e^+e^-g$, $q^*g^* \rightarrow e^+e^-q$ subprocesses have been evaluated.

A reasonably good description of CMS and ATLAS experimental data for the inclusive prompt photon production at LHC and CDF and D0 data for the lepton pair production at Tevatron has been obtained. A theoretical uncertainties investigation has been studied and a predictive power of the used approach has been shown. We are ready to start the description of the Drell-Yan pair production at LHC.

It will be interesting to see new LHCb experimental data at large rapidity, since the lepton pair production in forward region corresponds to very small x , up to 10^{-6} .

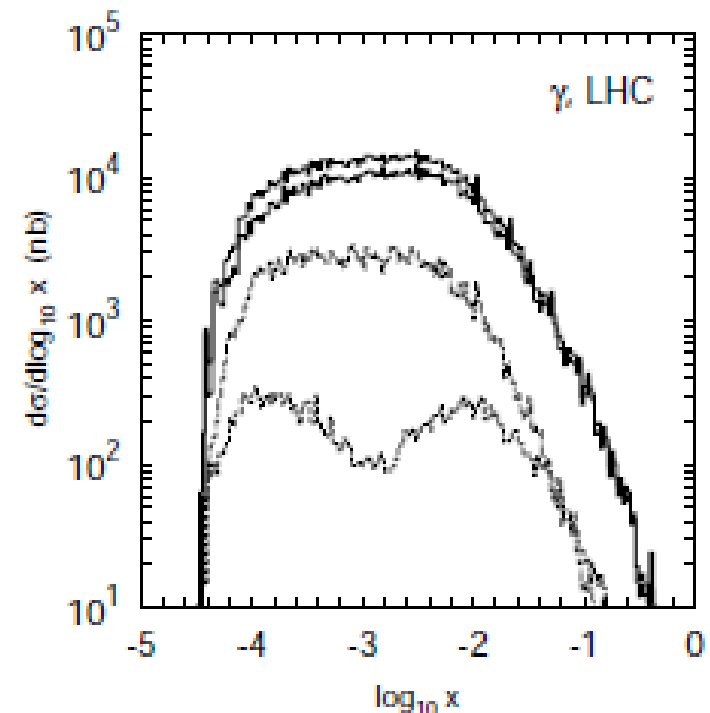
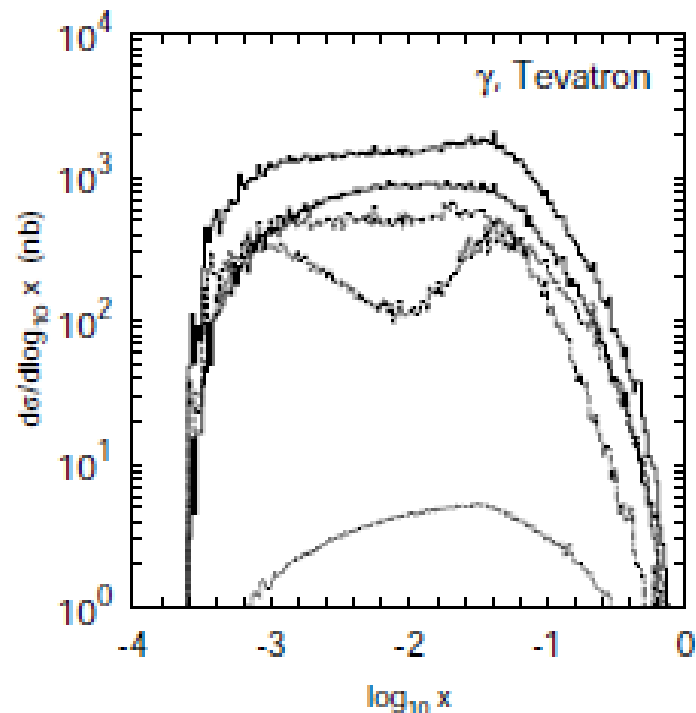
Back up

Numerical results



B1. Differential cross section of inclusive prompt photon production $pp \rightarrow \gamma X$ at LHC energies ($\sqrt{S}=7$ TeV). Comparison of the results obtained by CCFM A0 distributions with and without the 'Reduced sea' contribution (calculated with KMR distributions) added. The experimental data are of CMS.

Numerical results



5. Different contributions to the inclusive prompt photon production at the Tevatron (left panel) and LHC (right panel). The solid, dashed and dotted histograms correspond to $g+g \rightarrow \gamma+q+\bar{q}$, $q^\nu+g \rightarrow \gamma+q$ and $q^\nu+q^\nu \rightarrow \gamma+g$ subprocesses. The dash-dotted histograms - the "reduced sea" component. The thick solid histograms - the sum of all contributions.

Off-shell quarks

In the presented work we used a method, described in the article [S.P. Baranov, A.V. Lipatov, N.P. Zotov, Phys. Rev **D** **81**, 094034 (2010)]. According to this method, the off-shell quark spin density matrix has the form (in the limit of zero masses):

$$\sum_s u^s(k) \bar{u}^s(k) = \not{x} \hat{P}$$

Here P is the momentum of the incoming proton.

This prescription gives us the correct on-shell limit.

Divergencies

We do not use the concept of fragmentation functions obviously. In our approach the effect of final state radiation is already included in calculations at the level of partonic subprocess matrix elements (we have a $2 \rightarrow 3$ rather than $2 \rightarrow 2$ subprocesses). But as in the traditional approach the calculated cross sections can be split into two pieces: the direct and fragmentation contributions. They depend from fragmentation scale μ^2 .

In our calculations μ is the invariant mass of the produced photon and any final quark and we restrict direct contribution to $\mu \geq M = 1\text{GeV}$ in order to eliminate the collinear divergences in the direct cross section. Then the mass of light quark m_q can be safely to zero. The numerical effects of M is really small. It is less important than other theoretical uncertainties (connected with choice of renormalization and factorization scales).